Optimized Realization of Fault-Tolerant Heteropolar Magnetic Bearings

Uhn Joo Na
Research Associate
e-mail: ujn2738@acs.tamu.edu

Alan Palazzolo
Professor

Texas A&M University,
Mechanical Engineering,
College Station, Texas 77843-3123

Flux coupling in heteropolar magnetic bearings permits remaining active coils to assume actions of failed coils to produce force resultants identical to the un-failed actuator. This fault-tolerant control usually reduces load capacity because the redistribution of the magnetic flux which compensates for the failed coils leads to premature saturation in the stator or journal. A distribution matrix of voltages which consists of a redefined biasing voltage vector and two control voltage vectors can be optimized in a manner that reduces the peak flux density. An elegant optimization method using the Lagrange multiplier is presented in this paper. The linearized control forces can be realized up to certain combination of 5 poles failed for the 8 pole magnetic bearing. Position stiffness and voltage stiffness are calculated for the fault-tolerant magnetic bearings. Simulations show that fault-tolerant control of the multiple poles failed magnetic bearings with a horizontal flexible rotor can be achieved with reduced load capacity. [S0739-3717(00)01103-X]

1 Introduction

Magnetic suspension offers a number of practical advantages over conventional bearings such as lower rotating friction losses, high speeds, elimination of the lubrication, operation at temperature extremes and in vacuum, long life, and quiet operation. Magnetic bearings offer adaptable bearing damping and stiffness which come from the control action. System parameters can be designed to avoid resonance in the operating speed or for optimum damping through resonances. An electromagnet is inherently attractive because of the pole arrangement. The closed loop control algorithm acts to reduce the centering current and force, as the shaft approaches the bearing center. Similarly, the current is increased as the shaft moves away from the bearing center. This creates an effective stiffness of the bearing, tending to hold the shaft in a centered position. The force in the magnets acting on the shaft is produced by signals proportional to a combination of the shaft displacement and velocity, producing the desired values of stiffness and damping.

A fault-tolerant control seeks to provide continued operation of the bearing when its power amplifiers or coils suddenly fail. The fluxes in a heteropolar magnetic bearing are strongly coupled. The coil currents are selected to produce desired force resultants in the x and y directions. The control currents must be redefined in the case of single or multiple control coil failures in order to produce the same force resultants. The determination of this redistribution matrix of currents is the central objective in the following fault-tolerant magnetic bearing analysis.

Lyons et al. [1] used a three control axis radial bearing structure with control algorithms for redundant force control and rotor position measurement. Therefore, if one of the coils fails, the control axis can be shut down while maintaining control. Fedigan et al. [2] reported a fault-tolerant digital controller designed to meet the demanding performance and reliability requirements of high-speed magnetic bearing applications. Maslen and Meeker [3] developed the bias current linearization method to accommodate the fault tolerance of magnetic bearings and showed that the redistribution matrix which linearizes control forces can be obtained even if one or more coils fail. The fault tolerant magnetic bearing system was demonstrated on a large flexible-rotor test rig [4].

Many researchers investigated load capacity of the magnetic bearing. Maslen et al. [5] presented an expression that describes a maximum bearing load. Bornstein [6] derived equations to express the dynamic load capacity. Rao et al. [7] showed that the stiffness capacity of a magnetic bearing can be described as a function of the ratio of dynamic and static loads.

The present paper extends the preceding work of Maslen and Meeker by minimizing the flux density vector norm to reduce the possibility of pole material saturation and yields current distribution matrices that are effective even for the case of 5 poles failed.

2 Determination of Redistribution Matrices for Minimization of the Flux Density Vector Euclidean Norm

The equivalent magnetic circuit of an 8-pole heteropolar radial magnetic bearing with 8 independent control currents is shown in Fig. 1.

Maslen and Meeker [3] developed equations from (1) to (4).

$$R(x,y)\,\phi(x,y)=N\boldsymbol{I} \tag{1}$$

$$B(x,y)=A^{-1}R(x,y)^{-1}N\boldsymbol{I}=V(x,y)\boldsymbol{I} \tag{2}$$

Magnetic forces can be then described as;

$$F_x(x,y)=-B(x,y)^T\frac{\partial D(x,y)}{\partial x}B(x,y) \tag{3}$$

$$F_y(x,y)=-B(x,y)^T\frac{\partial D(x,y)}{\partial y}B(x,y), \tag{4}$$

where

$$D(x,y)=diag(g_j(x,y)a_j/(2\mu_0)) \tag{5}$$

$$g_j(x,y)=g_0-x\cos\theta_j-y\sin\theta_j \tag{6}$$

Maslen and Meeker [3] presented the necessary conditions for the bias current linearization for the fault-tolerant magnetic bearings, which are described as;

$$\hat{T}^TG_x(x,y)\hat{T}=M_x \tag{7}$$

$$\hat{T}^TG_y(x,y)\hat{T}=M_y, \tag{8}$$

where

$$G_x(x,y)=-K^TV(x,y)^T\frac{\partial D(x,y)}{\partial x}V(x,y)K \tag{9}$$

Contributed by the Technical Committee on Vibration and Sound for publication in the JOURNAL OF VIBRATION AND ACOUSTICS. Manuscript received Sept. 1999; revised Jan. 2000. Associate Technical Editor: J. Q. Sun.

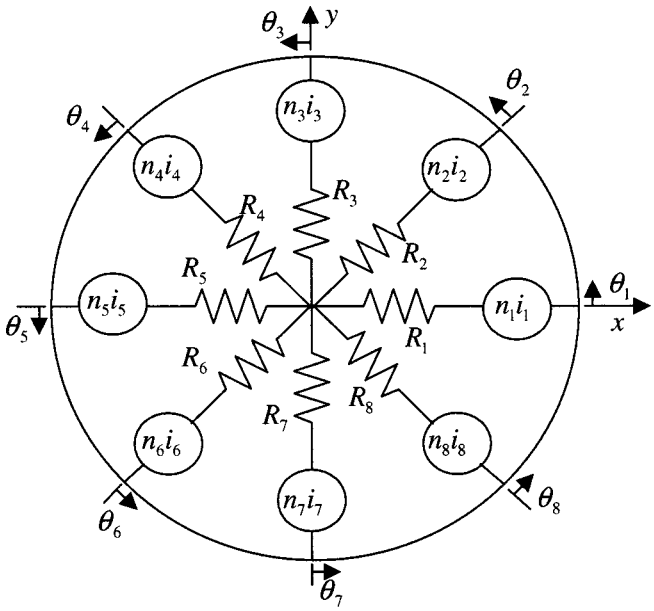

Fig. 1 Eight pole heteropolar equivalent magnetic circuit

$$G_y(x,y) = -K^T V(x,y)^T \frac{\partial D(x,y)}{\partial y} V(x,y) K \tag{10}$$

$$M_x = \begin{bmatrix} 0 & 0.5 & 0 \\ 0.5 & 0 & 0 \\ 0 & 0 & 0 \end{bmatrix} \tag{11}$$

$$M_y = \begin{bmatrix} 0 & 0 & 0.5 \\ 0 & 0 & 0 \\ 0.5 & 0 & 0 \end{bmatrix} \tag{12}$$

Maslen and Meeker [3] suggested a method to obtain useful solutions to Eqs. (7) and (8). One of the criteria to decide which solution to use is to find the solution of $\hat{T}$ which minimizes the peak flux density, so the maximum load capacity should be obtained before the magnetic bearing saturates. Meeker [8] suggested that the Reduced Gradient method could give good solutions. Maslen et al. [4] reported that the greatest failures that this stator can tolerate are certain configurations involving four failed coils, and that it is not possible to realize the redistribution matrix with four adjacent coils failed.

An alternative optimization method to minimize the norm of B is presented in this paper. It is assumed that the orientation of the desired forces is fixed to θ and the rotor is at an arbitrary position, then the B is only a function of $\hat{T}$. The cost function is;

$$J(\hat{T}) = B(\hat{T})^T B(\hat{T}) = I^T V^T V I, \tag{13}$$

$$\text{where} \qquad I = TV_c = K\hat{T}\boldsymbol{V}_c \tag{14}$$

$$\boldsymbol{V}_c = [v_b, v_{cx}, v_{cy}]^T \tag{15}$$

Magnetic forces of Eqs. (3) and (4) are in the form of weighted Euclidean norm of the flux density vectors. The peak flux density may be reduced by minimizing the Euclidean norm of flux density vector. In this manner, the best solution $\hat{T}$ is what minimizes $J(\hat{T})$. Substituting Eqs. (2), (7), (8), (11), (12), (14), and (15) into Eqs. (3) and (4) leads to

$$F_x = v_b v_{cx} \tag{16}$$

$$F_y = v_b v_{cy} \tag{17}$$

Therefore, magnetic forces are completely decoupled and linearized even in case of failed control coils if the necessary conditions (7) and (8) are met with appropriate $\hat{T}$. The basic problem is to obtain the $\hat{T}$ that satisfies

$$\min J(\hat{T}) \tag{18}$$

subject to the constraints;

$$\hat{T}^T G_x(x,y)\hat{T} - M_x = \underline{0} \tag{19}$$

$$\hat{T}^T G_y(x,y)\hat{T} - M_y = \underline{0}, \tag{20}$$

$$\text{where} \qquad \hat{T} = [\hat{\boldsymbol{T}}_b \hat{\boldsymbol{T}}_x \hat{\boldsymbol{T}}_y] \tag{21}$$

$$\hat{\boldsymbol{T}}_b = [t_1, t_2, \ldots, t_{m-1}, t_m]^T \tag{22}$$

$$\hat{\boldsymbol{T}}_x = [t_{m+1}, t_{m+2}, \ldots, t_{2m-1}, t_{2m}]^T \tag{23}$$

$$\hat{\boldsymbol{T}}_y = [t_{2m+1}, t_{2m+2}, \ldots, t_{3m-1}, t_{3m}]^T \tag{24}$$

Equations (19) and (20) can be rewritten in 18 scalar forms. Since G_x and G_y are symmetric, those 18 equations can be reduced to 12 equality constraint equations.

$$h_1(\hat{T}) = \hat{\boldsymbol{T}}_b^T G_x \hat{\boldsymbol{T}}_b = 0 \tag{25}$$

$$h_2(\hat{T}) = \hat{\boldsymbol{T}}_b^T G_x \hat{\boldsymbol{T}}_x - 0.5 = 0 \tag{26}$$

$$h_3(\hat{T}) = \hat{\boldsymbol{T}}_b^T G_x \hat{\boldsymbol{T}}_y = 0 \tag{27}$$

$$h_4(\hat{T}) = \hat{\boldsymbol{T}}_x^T G_x \hat{\boldsymbol{T}}_x = 0 \tag{28}$$

$$h_5(\hat{T}) = \hat{\boldsymbol{T}}_x^T G_x \hat{\boldsymbol{T}}_y = 0 \tag{29}$$

$$h_6(\hat{T}) = \hat{\boldsymbol{T}}_y^T G_x \hat{\boldsymbol{T}}_y = 0 \tag{30}$$

$$h_7(\hat{T}) = \hat{\boldsymbol{T}}_b^T G_y \hat{\boldsymbol{T}}_b = 0 \tag{31}$$

$$h_8(\hat{T}) = \hat{\boldsymbol{T}}_b^T G_y \hat{\boldsymbol{T}}_x = 0 \tag{32}$$

$$h_9(\hat{T}) = \hat{\boldsymbol{T}}_b^T G_y \hat{\boldsymbol{T}}_y - 0.5 = 0 \tag{33}$$

$$h_{10}(\hat{T}) = \hat{\boldsymbol{T}}_x^T G_y \hat{\boldsymbol{T}}_x = 0 \tag{34}$$

$$h_{11}(\hat{T}) = \hat{\boldsymbol{T}}_x^T G_y \hat{\boldsymbol{T}}_y = 0 \tag{35}$$

$$h_{12}(\hat{T}) = \hat{\boldsymbol{T}}_y^T G_y \hat{\boldsymbol{T}}_y = 0 \tag{36}$$

The Lagrange Multiplier method can be applied on the basic problem to solve for $\hat{T}$ that satisfies Eqs. (19) and (20). Define:

$$L(\hat{T}) = B(\hat{T})^T B(\hat{T}) + \sum_{j=1}^{12} \lambda_i h_j(\hat{T}) \tag{37}$$

Partial differentiation of Eq. (37) with respect to t_i and λ_j leads to $3m+12$ nonlinear algebraic equations to solve for t_i and λ_j.

$$f_i = \frac{\partial L}{\partial t_i} = 0, \quad i = 1,2,\ldots,3m \tag{38}$$

$$f_{j+3m} = h_j(\hat{T}) = 0, \quad j = 1,2,\ldots,12 \tag{39}$$

A vector form of $3m+12$ nonlinear algebraic equations is;

$$F(t,\lambda) = \begin{bmatrix} f_1(t,\lambda) \\ f_2(t,\lambda) \\ \cdot \\ \cdot \\ \cdot \\ f_{3m+11}(t,\lambda) \\ f_{3m+12}(t,\lambda) \end{bmatrix} = \begin{bmatrix} 0 \\ 0 \\ \cdot \\ \cdot \\ \cdot \\ 0 \\ 0 \end{bmatrix} \tag{40}$$

Equation (40) can be solved for t_i and λ_j numerically by any nonlinear algebraic equation solver. A nonlinear algebraic equation solver using a least square iterative method (MATLAB) was used to solve Eq. (40) numerically. Since the cost function is not convex and equality constraints are not affine, there may exist multiple local optima. Various initial guess of t and λ may be tested in order to find a better solution of $\hat{T}$. Local minima are guaranteed and also global minimum can be obtained if an effective global minimum searching algorithm is used. The Jacobian matrix of $F(t,\lambda)$ becomes increasingly poorly conditioned, as the algorithm converges on a solution. However, the algorithm can converge quite close to a valid $\hat{T}$ that satisfies Eq. (40) without the Jacobian becoming singular. Another feature of the Lagrange Multiplier method is that it introduces Lagrange Multiplier unknowns, λ, and makes the system of equations square (same number of equations and unknowns) for any failure case. In case of the 5 poles failed bearing, equality constraint equations have only 9 unknowns with 12 equations. It is then difficult to solve those equations directly. However, 21 nonlinear algebraic equations with 12 Lagrange Multiplier unknowns and 9 distribution matrix unknowns can be solved for t_i and λ_j.

Nonsingular $\hat{T}$ for the 5 poles failed bearing is nonexistent. For example, G_x for 2-4-6-7-8th poles failed bearing is of full rank, and G_y is a matrix of rank 2. G_x is not congruent with M_x. However, singular $\hat{T}$ that satisfies Eqs. (7) and (8) may exist. Maslen and Meeker [3] and Meeker [8] showed that the conditions for generating the two orthogonal arbitrary forces from the failed bearing are:

(1) G_x and G_y should be indefinite.

(2) There exists any $\hat{T}$ which satisfy Eqs. (7) and (8).

Hence $\hat{T}$ being nonsingular is not a requirement for realizing the desired forces. It is notable that the congruence relation is also not satisfied for failure cases other than the 5 poles failed case. For example, for the 4 poles failed case (3-6-7-8th poles failed) a pseudo-distribution matrix may be formulated as;

$$T_1=\begin{bmatrix} T_{b1} & T_{x1} & T_{y1} & T_{d1} \\ T_{b2} & T_{x2} & T_{y2} & T_{d2} \\ T_{b3} & T_{x3} & T_{y3} & T_{d3} \\ T_{b4} & T_{x4} & T_{y4} & T_{d4} \end{bmatrix} \tag{41}$$

Then

$$T_1^T G_x T_1=\begin{bmatrix} 0 & 0.5 & 0 & 0 \\ 0.5 & 0 & 0 & 0 \\ 0 & 0 & 0 & 0 \\ 0 & 0 & 0 & 0 \end{bmatrix} \tag{42}$$

$$T_1^T G_y T_1=\begin{bmatrix} 0 & 0 & 0.5 & 0 \\ 0 & 0 & 0 & 0 \\ 0.5 & 0 & 0 & 0 \\ 0 & 0 & 0 & 0 \end{bmatrix} \tag{43}$$

should hold. T_d's do not affect the Eqs. (7) and (8). Since G_x is a matrix of rank 4 and G_y is a matrix of rank 3, a nonsingular T_1 does not exist. T_1 should be a matrix of rank 2 to satisfy Eqs. (42) and (43). Dummy variables T_d's can be truncated from T_1 to obtain the solution $\hat{T}$.

3 Optimal Solutions of 8 Pole Heteropolar Magnetic Bearing

The 8-pole heteropolar magnetic bearing used in this analysis has uniform pole face area of $4.91\times10^{-4}\,\mathrm{m}^2$, a nominal gap of 0.001 m, and 200 turn coils. Equation (40) was solved numerically for some selected combinations of failure cases from 3 poles to 5 poles failure. Some of the example distribution matrices were excerpted from the previous works [3], and were compared with distribution matrices calculated by the Lagrange Multiplier method. $3m+12$ nonlinear algebraic equations are solved for the $\hat{T}$ that minimizes flux density vector Euclidean norm. The flux density vector is described as;

$$\boldsymbol{B}(T)=B_b+B_x+B_y=VK\hat{T}_b v_b+VK\hat{T}_x v_{cx}+VK\hat{T}_y v_{cy} \tag{44}$$

Maslen and Meeker's T matrix for 6-7-8th poles failed magnetic bearing is shown in Eq. (45).

$$T=\begin{bmatrix} -0.198531 & -0.146643 & 0.172692 \\ -0.052334 & 0.022060 & 0.267589 \\ 0.034700 & -0.000865 & 0.338018 \\ -0.078408 & -0.012076 & 0.269612 \\ -0.198333 & 0.148658 & 0.156481 \\ 0 & 0 & 0 \\ 0 & 0 & 0 \\ 0 & 0 & 0 \end{bmatrix} \tag{45}$$

The T matrix for 6-7-8th poles failed magnetic bearing by the Lagrange Multiplier method is shown in Eq. (46).

$$T=\begin{bmatrix} -0.19853 & -0.14695 & 0.15198 \\ -0.052535 & -0.06403 & 0.30332 \\ 0.032217 & -4.1\,10^{-5} & 0.34364 \\ -0.052425 & 0.063943 & 0.30334 \\ -0.19852 & 0.14691 & 0.15206 \\ 0 & 0 & 0 \\ 0 & 0 & 0 \\ 0 & 0 & 0 \end{bmatrix} \tag{46}$$

Several local minima were found when various initial guess t and λ were tested. Equation (46) is the best solution among the solutions found. The global minimum searching method was not used in this analysis. One more Maslen and Meeker's T matrix for selected combination of 4-6-7-8th poles failed case is shown in Eq. (47).

$$T=\begin{bmatrix} 1.826025 & 0.012223 & -0.059953 \\ 0.108760 & -0.013794 & -0.038409 \\ -0.063425 & 0.006560 & -0.058641 \\ 0 & 0 & 0 \\ 1.802976 & -0.015078 & -0.051954 \\ 0 & 0 & 0 \\ 0 & 0 & 0 \\ 0 & 0 & 0 \end{bmatrix} \tag{47}$$

The T matrix for the 4-6-7-8th poles failed case calculated by the Lagrange Multiplier method is shown in Eq. (48).

$$T=\begin{bmatrix} 0.52228 & 0.05715 & -0.16355 \\ 0.22325 & 0.0371 & -0.09705 \\ -0.037124 & 0.0061 & -0.19255 \\ 0 & 0 & 0 \\ 0.50482 & -0.0524 & -0.1482 \\ 0 & 0 & 0 \\ 0 & 0 & 0 \\ 0 & 0 & 0 \end{bmatrix} \tag{48}$$

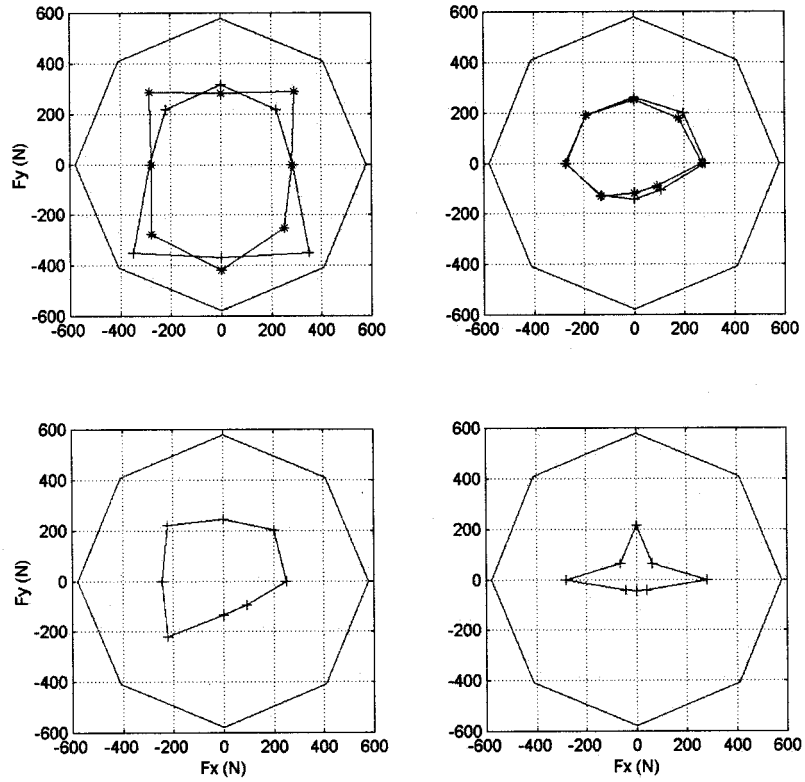

Fig. 2 Load capacity of the fault tolerant magnetic bearing for 6-7-8th coil failed(Upper Left), 4-6-7-8th coil failed (upper right), 5-6-7-8th coil failed (bottom left), and 2-4-6-7-8th coil failed (bottom right)

The T matrix for any combination of failed poles up to 4 out of 8 poles can be calculated by the Lagrange Multiplier method. For instance T for 4 adjacent poles failed (5-6-7-8th) is shown in Eq. (49).

$$T=\begin{bmatrix} -0.70668 & 0.061757 & 0.3218 \\ -0.29382 & 0.17041 & 0.29392 \\ -0.29166 & 0.082044 & \\ 0.34761 & & \\ -0.70677 & 0.154 & 0.28328 \\ 0 & 0 & 0 \\ 0 & 0 & 0 \\ 0 & 0 & 0 \\ 0 & 0 & 0 \end{bmatrix} \tag{49}$$

Though 5 poles fail, T can be calculated by the Lagrange Multiplier method except for two cases. T cannot be found if 5 adjacent poles are failed, or 4 adjacent poles and one more pole are failed. T for 2-4-6-7-8th poles failed case is shown in Eq. (50).

$$T=\begin{bmatrix} 0.85207 & 0.03172 & -0.23458 \\ 0 & 0 & 0 \\ 0 & 0 & -0.1902 \\ 0 & 0 & 0 \\ 0.85207 & -0.031681 & -0.23458 \\ 0 & 0 & 0 \\ 0 & 0 & 0 \\ 0 & 0 & 0 \end{bmatrix} \tag{50}$$

If less than three currents are controlled, T cannot be found. These conclusions are based on the authors' experience with convergence of the solver. Calculated T matrices should satisfy Eqs. (7) and (8). Least square iterative algorithm converges to T that nearly satisfy Eqs. (7) and (8), before the Jacobian matrix of $F(t,\lambda)$ becomes singular. Therefore, there exist some off-diagonal error terms in M matrices. Load capacity of the magnetic bearing with distribution matrices is calculated for 8 force directions. The load capacity of the fault-tolerant magnetic bearing can be calculated in a manner that the maximum component of B_b should be set to $b_{sat}/2$ by manipulating v_b and then B_x or B_y is increased or decreased until B reaches b_{sat} of 1.2 Tesla. Load capacity plots of the 4 failure cases are shown in Fig. 2. For 6-7-8th coil failed case minimum load capacity occurs at x directions for both Meeker's solution and the Lagrange Multiplier solution. However, load capacity of the Lagrange Multiplier solution along positive y direction (opposite to gravity direction) is 12 percent larger than that of Meeker's. For 4-6-7-8th coil failed case minimum load capacity of 143 N occurs at negative y direction. Load capacities of 5-6-7-8th coil failed case and 2-4-6-7-8th coil failed case are also determined for the distribution matrices of Eqs. (49) and (50). Load capacity of the 2-4-6-7-8th coil failed magnetic bearing is reduced to 44 N along the negative y direction. However, it shows that even the 5 coils failed bearing still can support considerable amount of gravity load (up to 200 N of magnetic force along the positive y direction).

4 Determination of Linearized Forces for Fault-Tolerant Magnetic Bearings

Valid T matrix can both linearize and decouple the multiple poles failed magnetic bearing forces. The distribution matrix of voltages, which consists of a redefined biasing voltage vector and two control voltage vectors, can be implemented in the controller.

The redistribution matrices for all failure cases can be implemented in a physical controller, so if some combinations of failures of the power amplifiers or coils are detected, the corresponding redistribution matrices can be switched at the same time. Linearized forces are defined in terms of a bias voltage and two control voltages. Nonlinear magnetic forces are defined as;

$$F_x(x,y) = I^T \frac{\partial U(x,y)}{\partial x} I \tag{51}$$

$$F_y(x,y) = I^T \frac{\partial U(x,y)}{\partial y} I \tag{52}$$

where

$$U(x,y) = V(x,y)^T D(x,y) V(x,y) \tag{53}$$

Partial derivative of $U(x,y)$ with respect to x derived as;

$$\frac{\partial U(x,y)}{\partial x} = V(x,y)^T \frac{\partial D(x,y)}{\partial x} V(x,y) + 2V(x,y) D(x,y) \frac{\partial V(x,y)}{\partial x} \tag{54}$$

An identity relation holds for the given $V(x,y)$ and $D(x,y)$:

$$V(x,y)^T \frac{\partial D(x,y)}{\partial x} V(x,y) = -V(x,y)^T D(x,y) \frac{\partial V(x,y)}{\partial x} \tag{55}$$

Equation (54) then becomes;

$$\frac{\partial U(x,y)}{\partial x} = -V(x,y)^T \frac{\partial D(x,y)}{\partial x} V(x,y) \tag{56}$$

Similarly, partial derivative of $U(x,y)$ with respect to y is derived as;

$$\frac{\partial U(x,y)}{\partial y} = -V(x,y)^T \frac{\partial D(x,y)}{\partial y} V(x,y) \tag{57}$$

Second partial derivatives of $U(x,y)$ with respect to x and y are described as;

$$\frac{\partial^2 U(x,y)}{\partial x^2} = -2V(x,y) \frac{\partial D(x,y)}{\partial x} \left(\frac{\partial V(x,y)}{\partial x} \right)^T \tag{58}$$

$$\frac{\partial^2 U(x,y)}{\partial y \partial x} = -2V(x,y) \frac{\partial D(x,y)}{\partial x} \left(\frac{\partial V(x,y)}{\partial y} \right)^T \tag{59}$$

$$\frac{\partial^2 U(x,y)}{\partial x \partial y} = -2V(x,y) \frac{\partial D(x,y)}{\partial y} \left(\frac{\partial V(x,y)}{\partial x} \right)^T \tag{60}$$

$$\frac{\partial^2 U(x,y)}{\partial y^2} = -2V(x,y) \frac{\partial D(x,y)}{\partial y} \left(\frac{\partial V(x,y)}{\partial y} \right)^T \tag{61}$$

The nonlinear magnetic forces in Eqs. (51) and (52) can also be linearized about the bearing center position and the zero control voltages by using Taylor series expansion.

$$F_x(x,y,v_{cx},v_{cy}) \approx \left.\frac{\partial F_x}{\partial x}\right|_{\substack{x=0\\y=0\\v_{cx}=0\\v_{cy}=0}} x + \left.\frac{\partial F_x}{\partial y}\right|_{\substack{x=0\\y=0\\v_{cx}=0\\v_{cy}=0}} y + \left.\frac{\partial F_x}{\partial v_{cx}}\right|_{\substack{x=0\\y=0\\v_{cx}=0\\v_{cy}=0}} v_{cx} + \left.\frac{\partial F_x}{\partial v_{cy}}\right|_{\substack{x=0\\y=0\\v_{cx}=0\\v_{cy}=0}} v_{cy} \tag{62}$$

$$F_y(x,y,v_{cx},v_{cy}) \approx \left.\frac{\partial F_y}{\partial x}\right|_{\substack{x=0\\y=0\\v_{cx}=0\\v_{cy}=0}} x + \left.\frac{\partial F_y}{\partial y}\right|_{\substack{x=0\\y=0\\v_{cx}=0\\v_{cy}=0}} y + \left.\frac{\partial F_y}{\partial v_{cx}}\right|_{\substack{x=0\\y=0\\v_{cx}=0\\v_{cy}=0}} v_{cx} + \left.\frac{\partial F_y}{\partial v_{cy}}\right|_{\substack{x=0\\y=0\\v_{cx}=0\\v_{cy}=0}} v_{cy} \tag{63}$$

The linearized force components in the right hand side of Eqs. (62) and (63) can be described as position stiffness and voltage stiffness. Position stiffness is described as;

$$\left.\frac{\partial F_x}{\partial x}\right|_{\substack{x=0\\y=0\\v_{cx}=0\\v_{cy}=0}} = -K_{pxx} = T_b^T \frac{\partial^2 U(x,y)}{\partial x^2} T_b v_b^2 \Big|_{\substack{x=0\\y=0}} = T_b^T U_{xx0} T_b v_b^2 \tag{64}$$

$$\left.\frac{\partial F_x}{\partial y}\right|_{\substack{x=0\\y=0\\v_{cx}=0\\v_{cy}=0}} = -K_{pxy} = T_b^T \frac{\partial^2 U(x,y)}{\partial y \partial x} T_b v_b^2 \Big|_{\substack{x=0\\y=0}} = T_b^T U_{xy0} T_b v_b^2 \tag{65}$$

$$\left.\frac{\partial F_y}{\partial x}\right|_{\substack{x=0\\y=0\\v_{cx}=0\\v_{cy}=0}} = -K_{pyx} = T_b^T \frac{\partial^2 U(x,y)}{\partial x \partial y} T_b v_b^2 \Big|_{\substack{x=0\\y=0}} = T_b^T U_{yx0} T_b v_b^2 \tag{66}$$

$$\left.\frac{\partial F_y}{\partial y}\right|_{\substack{x=0\\y=0\\v_{cx}=0\\v_{cy}=0}} = -K_{pyy} = T_b^T \frac{\partial^2 U(x,y)}{\partial y^2} T_b v_b^2 \Big|_{\substack{x=0\\y=0}} = T_b^T U_{yy0} T_b v_b^2 \tag{67}$$

The amplitudes of the current inputs for the fault-tolerant bearing are usually not uniform, so it is difficult to define current stiffness for the multiple poles failed bearing. Instead voltage stiffness is defined as:

$$\left.\frac{\partial F_x}{\partial v_{cx}}\right|_{\substack{x=0\\y=0\\v_{cx}=0\\v_{cy}=0}} = K_{vxx} = \frac{\partial F_x}{\partial V_c} \left.\frac{\partial V_c}{\partial v_{cx}}\right|_{\substack{x=0\\y=0\\v_{cx}=0\\v_{cy}=0}} = 2T_b^T \frac{\partial U(x,y)}{\partial x} T_x v_b \Big|_{\substack{x=0\\y=0}} = 2T_b^T U_{x0} T_x v_b \tag{68}$$

$$\left.\frac{\partial F_x}{\partial v_{cy}}\right|_{\substack{x=0\\y=0\\v_{cx}=0\\v_{cy}=0}} = K_{vxy} = \frac{\partial F_x}{\partial V_c} \left.\frac{\partial V_c}{\partial v_{cy}}\right|_{\substack{x=0\\y=0\\v_{cx}=0\\v_{cy}=0}} = 2T_b^T \frac{\partial U(x,y)}{\partial x} T_y v_b \Big|_{\substack{x=0\\y=0}} = 2T_b^T U_{x0} T_y v_b \tag{69}$$

$$\left.\frac{\partial F_y}{\partial v_{cx}}\right|_{\substack{x=0\\y=0\\v_{cx}=0\\v_{cy}=0}} = K_{vyx} = \frac{\partial F_y}{\partial V_c} \left.\frac{\partial V_c}{\partial v_{cx}}\right|_{\substack{x=0\\y=0\\v_{cx}=0\\v_{cy}=0}} = 2T_b^T \frac{\partial U(x,y)}{\partial y} T_x v_b \Big|_{\substack{x=0\\y=0}} = 2T_b^T U_{y0} T_x v_b \tag{70}$$

$$\left.\frac{\partial F_y}{\partial v_{cy}}\right|_{\substack{x=0\\y=0\\v_{cx}=0\\v_{cy}=0}} = K_{vyy} = \frac{\partial F_y}{\partial V_c} \left.\frac{\partial V_c}{\partial v_{cy}}\right|_{\substack{x=0\\y=0\\v_{cx}=0\\v_{cy}=0}} = 2T_b^T \frac{\partial U(x,y)}{\partial y} T_y v_b \Big|_{\substack{x=0\\y=0}} = 2T_b^T U_{y0} T_y v_b \tag{71}$$

The position stiffness and voltage stiffness are calculated for the distribution matrices of Eqs. (46), (48), (49), and (50) at the center position of the bearing. The bias voltage gains are adjusted for the distribution matrices so that the maximum component of the bias flux density vector should be equal to $b_{sat}/2$. The calculated position stiffness and voltage stiffness and bias voltage gain are shown in Table 1.

Since T is calculated for decoupled linearized forces, the cross-coupled voltage stiffness terms should be negligibly small for a valid T. However, there exist some cross-coupled position stiffnesses because the flux densities are unevenly distributed in case of the calculated distribution matrix for the multiple coils failed magnetic bearing. Figure 3 shows that the rotor is pulled to the right while levitating when the static load of 123 N is applied on the fault-tolerant magnetic bearing. Decoupled linearized magnetic forces are then described as;

Table 1 The calculated stiffness for the fault-tolerant magnetic bearing

	Eq. (46)	Eq. (48)	Eq. (49)	Eq. (50)
v_b	17.3	6.5	7.4	3.8
K_{pxx} (N/m)	-314490	-307930	-564110	-323430
K_{pxy} (N/m)	8.477	12077	209760	0
K_{pyx} (N/m)	8.477	12077	209760	0
K_{pyy} (N/m)	-110690	-97887	-144830	-64686
K_{vxx} (N/Volt)	17.3	6.5	7.4	3.8
K_{vxy} (N/Volt)	-0.0001	-0.0018	0.000438	0
K_{vyx} (N/Volt)	-0.00001	0.00048	-0.00017	0
K_{vyy} (N/Volt)	17.3	6.5	7.4	3.8

$$F_x = -K_{pxx}x - K_{pxy}y + K_{vxx}v_{cx} \tag{72}$$

$$F_y = -K_{pyx}x - K_{pyy}y + K_{vyy}v_{cy} \tag{73}$$

The linearized forces are used to design a control law so that the closed loop should be stabilized.

5 Control System Design

A fault-tolerant magnetic bearing test rig with a horizontal flexible rotor was built at NASA Glenn. The flexible rotor has mass of 10.7 kg length of 0.69 m, and bearing location of 0.1235 m from the ends. A finite element model of the flexible rotor with 38 elements is shown in Fig. 4.

The flexible rotor is discritized into a reasonable number of elements which consist of a series of massless beam elements and lumped mass and inertias. Palazzolo [9] shows a general n disc rotor model with cylindrical beam elements based on Euler's assumptions. The mass, polar moment of inertia, and transverse moment of inertia are halved and placed at each node. The equation of motion for the flexible rotor is then described as;

$$\underline{M}\ddot{X}(t) + \underline{G}\dot{X}(t) + \underline{K}X(t) = \boldsymbol{F}_s(t), \tag{74}$$

where $\underline{M}$, $\underline{G}$, and $\underline{K}$ represent mass, gyroscopic moment, and stiffness matrices respectively. External forces exerted on the system of equations are described as;

$$\boldsymbol{F}_s(t) = \boldsymbol{F}_{mag}(t) + \boldsymbol{F}_{grav} + \boldsymbol{F}_u(t), \tag{75}$$

where $\boldsymbol{F}_{mag}$, $\boldsymbol{F}_{grav}$, and $\boldsymbol{F}_u$ represent magnetic force, gravity force, and unbalance force vectors respectively. The first order form of the system of equations is:

$$\begin{bmatrix} \ddot{X}(t) \\ \dot{X}(t) \end{bmatrix} = \begin{bmatrix} -\underline{M}^{-1}\underline{G} & -\underline{M}^{-1}\underline{K} \\ \underline{I} & \underline{0} \end{bmatrix} \begin{bmatrix} \dot{X}(t) \\ X(t) \end{bmatrix} + \begin{bmatrix} \underline{M}^{-1} \\ \underline{0} \end{bmatrix} \boldsymbol{F}_s(t) \tag{76}$$

or

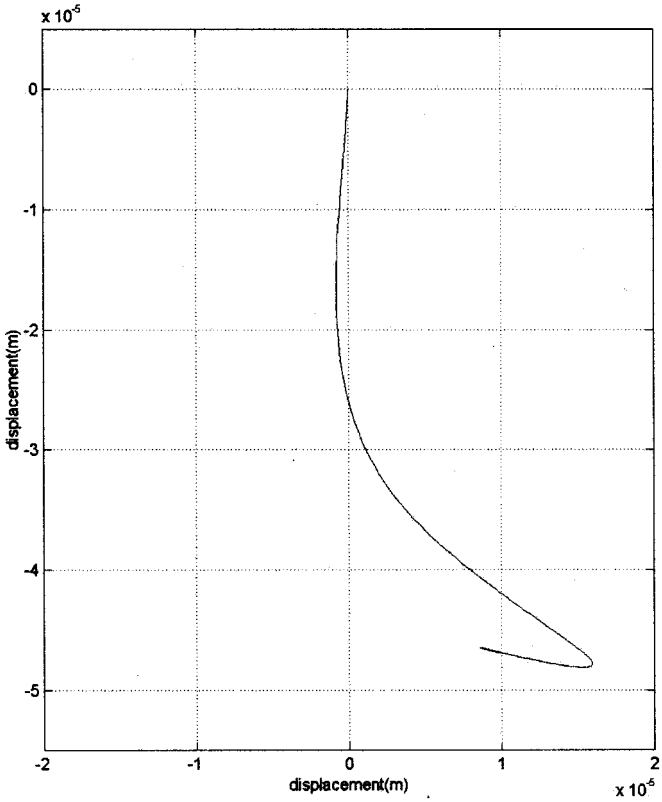

Fig. 3 Static deflection of the rotor for the 5-6-7-8th coils failed magnetic bearing

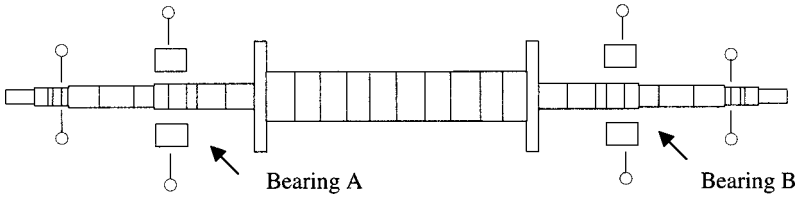

Fig. 4 Finite element model of the flexible rotor

$$\dot{Z}(t)=\underline{A}_P Z(t)+\underline{B}_P F_s(t) \tag{77}$$

A vector form of the magnetic bearing forces applied on the rotor system is described as;

$$F_{mag}(t)=H\overline{F}(t), \tag{78}$$

where

$$\overline{F}(t)=\begin{bmatrix} F_x^A(t) \\ F_y^A(t) \\ F_x^B(t) \\ F_y^B(t) \end{bmatrix} \tag{79}$$

where H is the 156×4 matrix which assigns magnetic forces to the corresponding states. F_x^A, F_y^A, F_x^B, and F_y^B are the nonlinear magnetic forces for Bearing *A* and *B*. Substituting Eqs. (72) and (73) into (79) leads to;

$$\overline{F}(t)=K_{\text{pos}}X_B+K_{vol}V_B, \tag{80}$$

where

$$X_B=[x^A,y^A,x^B,y^B]^T \tag{81}$$

$$V_B=[v_{cx}^A,v_{cy}^A,v_{cx}^B,v_{cy}^B]^T \tag{82}$$

The control voltages are described as;

$$v_{cx}(t)=-k_{px}v_{sx}(t)-k_{dx}\dot{v}_{sx}(t) \tag{83}$$

$$v_{cy}(t)=-k_{py}v_{sy}(t)-k_{dy}\dot{v}_{sy}(t), \tag{84}$$

where $v_{sx}(t)$, $v_{sy}(t)$ represent the sensor voltages. The sensor voltage vector is given as;

$$\begin{bmatrix} v_{sx}^A(t) \\ v_{sy}^A(t) \\ v_{sx}^B(t) \\ v_{sy}^B(t) \end{bmatrix}=\kappa_s\begin{bmatrix} x_s^A(t) \\ y_s^A(t) \\ x_s^B(t) \\ y_s^B(t) \end{bmatrix}=\kappa_s S\,X(t) \tag{85}$$

κ_s is the sensor sensitivity. S is the 4×156 matrix which assigns sensor target locations to the corresponding states. If sensors are collocated with magnetic actuators, S becomes H^T. Substituting Eqs. (83)–(84) into (82) leads to;

$$V_B=K_P H^T X+K_D H^T\dot{X} \tag{86}$$

Equation (78) then becomes;

$$F_{mag}=H(K_{pos}+K_P)H^T X+HK_D H^T\dot{X} \tag{87}$$

The closed loop equation is:

$$\dot{Z}(t)=A_{cl}Z+B_p(F_{grav}+F_u) \tag{88}$$

where

$$A_{cl}=\begin{bmatrix} -\underline{M}^{-1}\underline{G}+HK_D H^T & -\underline{M}^{-1}\underline{K}+H(K_{pos}+K_P)H^T \\ \underline{I} & \underline{0} \end{bmatrix} \tag{89}$$

The closed loop dynamics may be stabilized by increasing k_p and k_d until the control force overcomes the negative position stiffness. Furthermore, the closed loop bearing stiffness and damping can be adjusted by tuning PD controller gains, k_p and k_d [10]. Rotor critical speeds and their corresponding dampings can be designed by tuning active bearing properties [11].

The first order form of the rotor system equation has 312 states. This will make the plant too large for simulation. Higher modes than 2000 Hz are rarely excited in the real world rotor system. Number of states in Eq. (74) is considerably reduced by using modal condensation. The first r modes of the system below 2000 Hz are selected and normalized as shown in Eq. (90).

$$\Psi_{156\times r}=[\Psi_1\ \ \Psi_2\ \ .\ \ .\ \ \Psi_r] \tag{90}$$

$r\times 1$ modal state vector v defined as:

$$X(t)=\Psi v(t) \tag{91}$$

Modal equation of motion for the flexible rotor is then described as:

$$\tilde{\underline{M}}\ddot{v}(t)+\tilde{\underline{G}}\dot{v}(t)+\tilde{\underline{K}}v(t)=\tilde{F}(t), \tag{92}$$

where

$$\tilde{\underline{M}}=\Psi^T\underline{M}\Psi \tag{93}$$

$$\tilde{\underline{K}}=\Psi^T\underline{K}\Psi \tag{94}$$

$$\tilde{\underline{G}}=\Psi^T\underline{G}\Psi \tag{95}$$

$$\tilde{F}(t)=\Psi^T F_s(t) \tag{96}$$

6 Simulations

Sensor dynamics and power amplifier dynamics are included in the closed loop path. Sensors have a sensitivity of 7874 V/m. A detailed outline of the fault-tolerant controller is shown in Fig. 5. The 8-pole heteropolar magnetic bearing used in the test rig has uniform pole face area of $6.02\times 10^{-4}\,\text{m}^2$, a nominal gap of $5.08\times 10^{-4}\,\text{m}$, and 50 turn coils. Equation (40) was solved for the 5-6-7-8th and the 2-4-6-7-8th poles failed cases. The T matrix for the un-failed bearing is excerpted from the previous work [3] as shown in Eq. (97).

$$T=\frac{g_0}{4n\sqrt{\mu_0 a}}\begin{bmatrix} 2 & 2\cos(0) & 2\sin(0) \\ -2 & -2\cos\left(\frac{\pi}{4}\right) & -2\sin\left(\frac{\pi}{4}\right) \\ 2 & 2\cos\left(\frac{2\pi}{4}\right) & 2\sin\left(\frac{2\pi}{4}\right) \\ -2 & -2\cos\left(\frac{3\pi}{4}\right) & -2\sin\left(\frac{3\pi}{4}\right) \\ 2 & 2\cos(\pi) & 2\sin(\pi) \\ -2 & -2\cos\left(\frac{5\pi}{4}\right) & -2\sin\left(\frac{5\pi}{4}\right) \\ 2 & 2\cos\left(\frac{6\pi}{4}\right) & 2\sin\left(\frac{6\pi}{4}\right) \\ -2 & -2\cos\left(\frac{7\pi}{4}\right) & -2\sin\left(\frac{7\pi}{4}\right) \end{bmatrix} \tag{97}$$

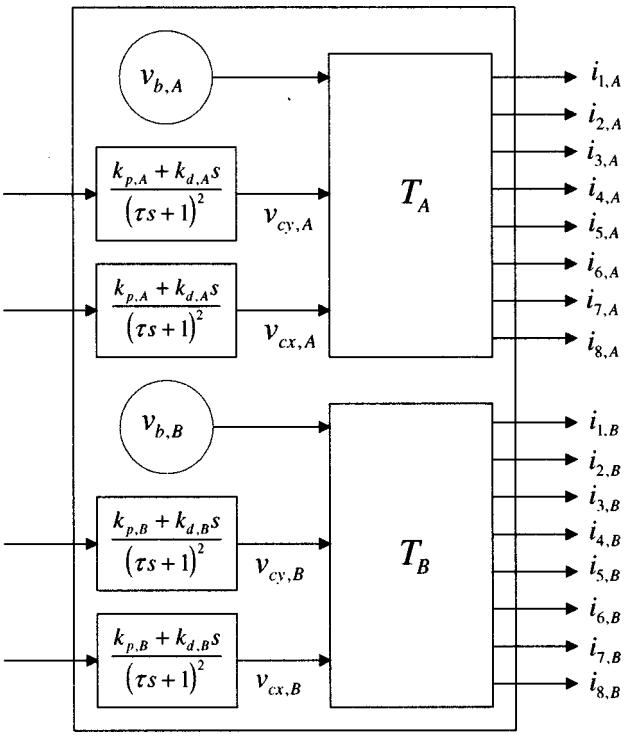

Fig. 5 Fault-tolerant control scheme

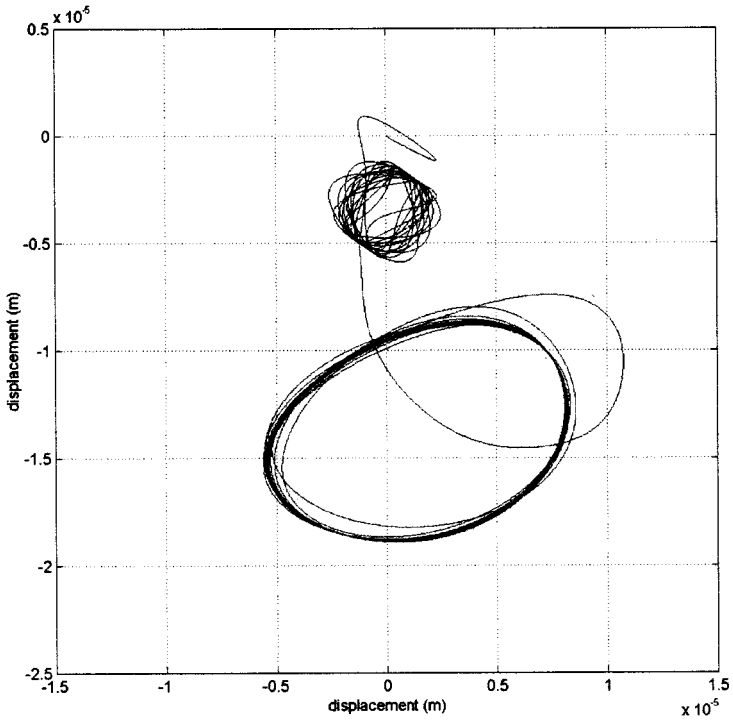

Fig. 6 Orbit plot for normal operation to the 5-6-7-8th poles failed operation

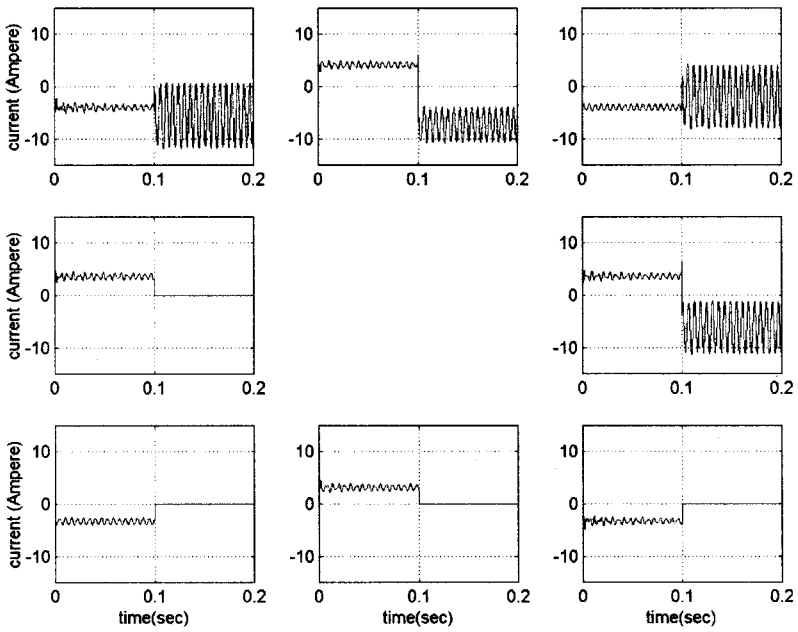

Fig. 7 Current inputs for normal operation to the 5-6-7-8th poles failed operation

The calculated T matrix for the 5-6-7-8th poles failed case is:

$$T=\begin{bmatrix} -10.398 & 0.01717 & 0.06897 \\ -4.9209 & 0.045068 & 0.057789 \\ -9.0257 & 0.031786 & 0.019684 \\ -9.5903 & 0.038636 & 0.0690.58 \\ 0 & 0 & 0 \\ 0 & 0 & 0 \\ 0 & 0 & 0 \\ 0 & 0 & 0 \end{bmatrix} \tag{98}$$

Equations (7) and (8) are satisfied with the calculated T as shown in Eqs. (99) and (100).

$$\hat{T}^T G_x \hat{T}=\begin{bmatrix} -4.107510^{-5} & 0.49999 & 2.510^{-6} \\ 0.49999 & -0.000164 & -0.001676 \\ 2.510^{-6} & -0.0001676 & 0.0016843 \end{bmatrix} \tag{99}$$

$$\hat{T}^T G_y \hat{T}=\begin{bmatrix} 2.2610^{-5} & 1.387910^{-7} & 0.49999 \\ 1.387910^{-7} & 0.0017771 & 0.00032816 \\ 0.49999 & 0.00032816 & 0.0008366 \end{bmatrix} \tag{100}$$

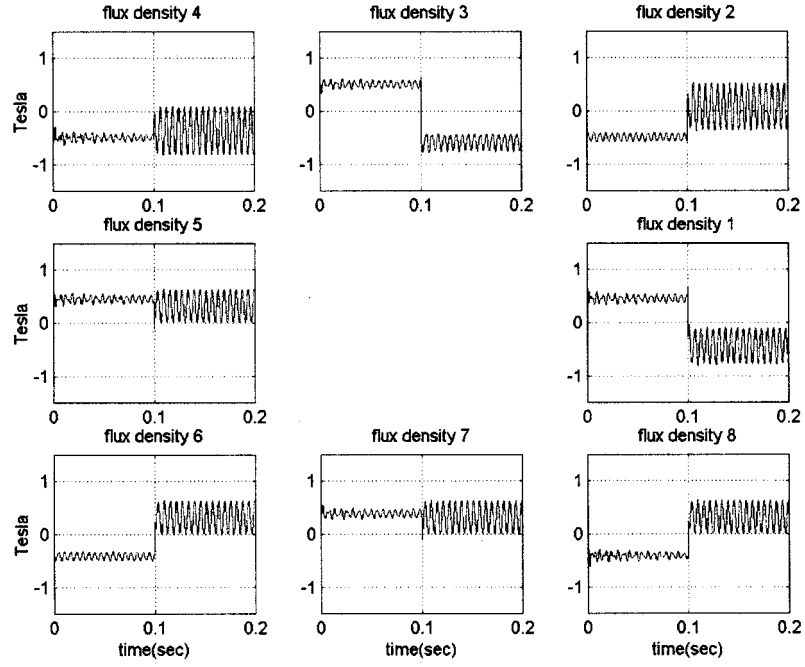

Fig. 8 Flux densities for normal operation to the 5-6-7-8th poles failed operation

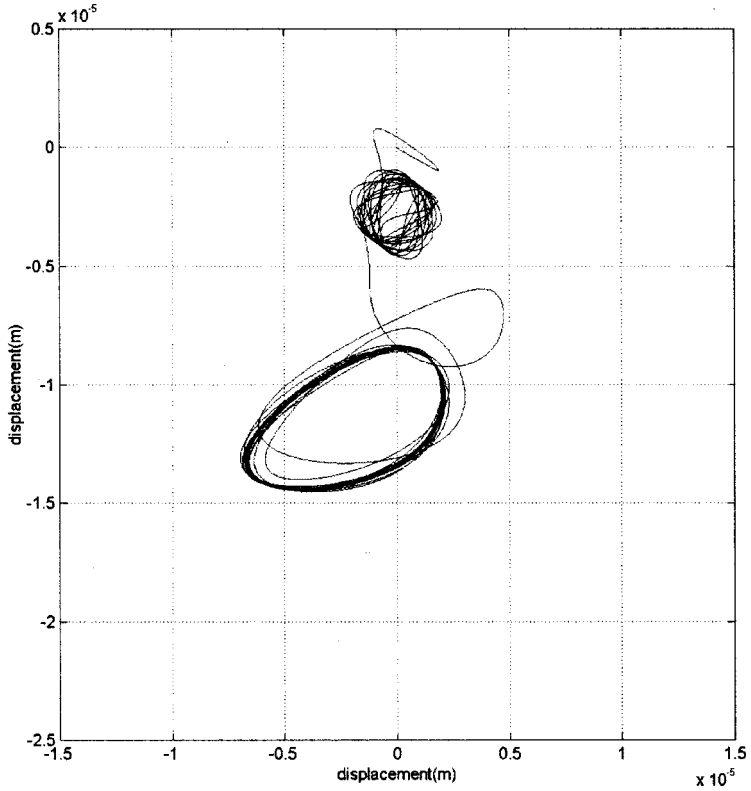

Fig. 9 Orbit plot for normal operation to the 2-4-6-7-8th poles failed operation

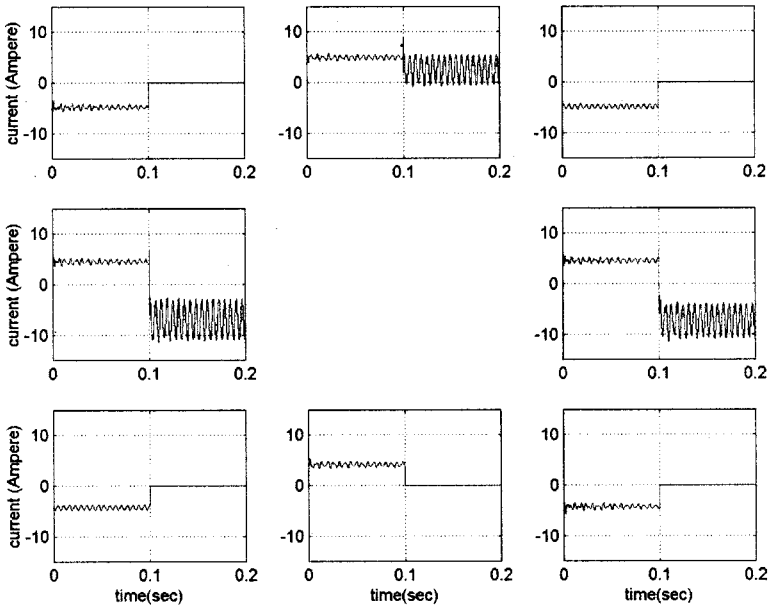

Fig. 10 Current inputs for normal operation to the 2-4-6-7-8th poles failed operation

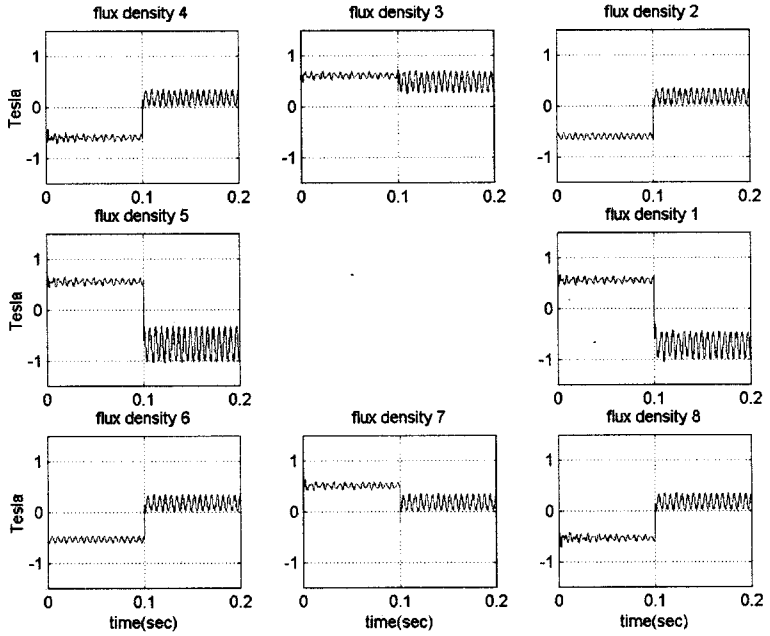

Fig. 11 Flux densities for normal operation to the 2-4-6-7-8th poles failed operation

The calculated T matrix for the 2-4-6-7-8th poles failed case is:

$$T=\begin{bmatrix} -11.49 & -0.0079149 & 0.058593 \\ 0 & 0 & 0 \\ -2.7316\,10^{-10} & 5.5249\,10^{-12} & 0.047502 \\ 0 & 0 & 0 \\ -11.49 & 0.0079169 & 0.058593 \\ 0 & 0 & 0 \\ 0 & 0 & 0 \\ 0 & 0 & 0 \end{bmatrix} \tag{101}$$

$$\hat{T}^T G_x \hat{T}=\begin{bmatrix} 1.239\,10^{-7} & 0.49999 & -3.673\,10^{-9} \\ 0.49999 & -4.334\,10^{-11} & -0.002205 \\ -3.673\,10^{-9} & -0.002205 & 2.999\,10^{-11} \end{bmatrix} \tag{102}$$

$$\hat{T}^T G_y \hat{T}=\begin{bmatrix} -5.750\,10^{-9} & 5.815\,10^{-11} & 0.49999 \\ 5.815\,10^{-11} & 2.286\,10^{-20} & -2.128\,10^{-11} \\ 0.49999 & -2.128\,10^{-11} & 0.001101 \end{bmatrix} \tag{103}$$

The linearized forces of Eqs. (72) and (73) are obtained for the

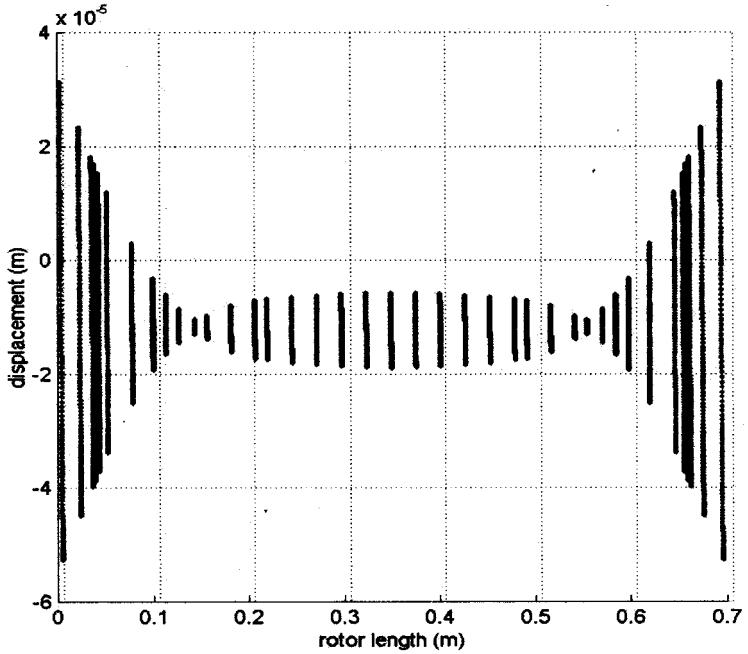

Fig. 12 Steady state rotor whirling for the 2-4-6-7-8th coil failed operation

5-6-7-8th poles failed at both bearings. Position and voltage stiffness, K_{pxx}, K_{pxy}, K_{pyy}, and K_{vxx} were -959640, 364350, -314430, and 0.9, respectively for v_b of 0.9. This shows that position stiffness along the y direction is much smaller than position stiffness along the x direction. Control gains of k_p and k_d for unfailed operation are selected as 100 and 0.2 respectively. Control gains of k_p and k_d for 4 poles failed operation are 450 and 1.5 respectively.

The transient response from normal operation with no failure to fault-tolerant control with 5-6-7-8th poles failed for both bearings was simulated for nonlinear bearings at 10,000 RPM. Unbalance eccentricity of $5.5\,10^{-6}$ m is applied at both rotor ends. A transient response orbit at bearing A is shown in Fig. 6. The orbit plot shows that the rotor sags slightly because of gravity. The rotor drops further while maintaining stable orbits when the 4 poles suddenly fail.

Transient response of the current inputs to bearing A for 5-6-7-8th poles failed case is shown in Fig. 7. Transient response of the flux densities in Bearing A is shown in Fig. 8.

The linearized forces are also obtained for the 2-4-6-7-8th poles failed at both bearings, and control gains of k_p and k_d are selected as 180 and 0.4 respectively. The position and voltage stiffness, K_{pxx}, K_{pxy}, K_{pyy}, and K_{vxx} were -1928400, 0, -385670, and 0.9, respectively for v_b of 0.9. The transient response from normal operation to fault-tolerant control with 2-4-6-7-8th poles failed for both bearings was also simulated for nonlinear bearings at 10,000 RMP. Transient response of the orbit at bearing A is shown in Fig. 9. Transient response of the current inputs to bearing A for the 2-4-6-7-8th poles failed case is shown in Fig. 10.

Spikes occur when the 5 poles are suddenly failed. However, currents can be stabilized with time. It is interesting to note that control current level is considerably increased after the failure while the rotor drops further down. Therefore, the load capacity is clearly reduced after the failure. If k_p is increased, the rotor will be lifted; however, this may saturate the power amplifier or magnetic bearing (whatever comes first) and limit the benefit of increasing the proportional gain. Transient response of the flux densities in Bearing A is shown in Fig. 11. This shows that the effects of increasing off-diagonal error terms in M_x and M_y barely affect the response, though maximum load capacity is reached. Steady state rotor whirling response after 5 coils are failed for both bearings are shown in Fig. 12.

7 Conclusions

General linearized magnetic forces for the heteropolar magnetic bearing are calculated with a fault-tolerant control scheme using a bias linearization method. Any one of the coil currents affects the flux in all of the air gaps. If one or more coils fail, a new coil current control scheme can be constructed which preserves the linear relationship between the required forces and coil currents. The calculation of a redistribution matrix of voltages which consists of a redefined biasing voltage vector and two control voltage vectors can be optimized in a manner that minimizes the flux density vector Euclidean norm. An elegant optimization method using a Lagrange Multiplier approach is presented in this paper. The redistribution matrix $\hat{T}$ is calculated with the Lagrange Multiplier method and compared with Maslen and Meeker's solutions. It is shown that $\hat{T}$ by the Lagrange Multiplier method has better performance in terms of reducing peak flux density. The desired control forces can be realized up to certain combination of 5 poles failed for the 8 pole magnetic bearing. Previous treatments of this problem in the literature yielded successful control only up to selected 4 failed poles for an 8-pole bearing. The position and voltage stiffness are derived from the fault-tolerant bearing and used for designing the closed loop control system.

Acknowledgments

The authors express their gratitude to Andrew Provenza, Ralph Jensen, Albert Kascak and Gerald Montague of the NASA Lewis-Dynamics Branch and Tom Calvert and Lynn Peterson of the NAVAL Surface Warfare Center - Carderock Division for sponsoring this research.

Nomenclature

A = pole face area matrix
a = pole face area
B = flux density vector
b_{sat} = saturation flux density
D = air gap energy matrix
F = magnetic force
g = air gap distance
G_x, G_y = reduced current to force matrices
h = equality constraint
$\boldsymbol{I}$ = current vector
v_b, v_{cx}, v_{cy} = bias, x control, and y control voltages
$\boldsymbol{V}_c$ = input voltage vector
$K_{pxx}, K_{pxy}, K_{pyx}, K_{pyy}$ = position stiffness
$K_{vxx}, K_{vxy}, K_{vyx}, K_{vyy}$ = voltage stiffness
K = current map matrix
K_{pos}, K_{vol} = position stiffness and voltage stiffness matrices respectively
K_P, K_D = proportional and derivative control gain matrices respectively
k_p, k_d = control gains
L = inductance matrix
m = number of active poles
M_x, M_y = separation matrices
N = coil turn matrix
n = number of coil turns
R = reluctance matrix
$\boldsymbol{T}_b, \boldsymbol{T}_x, \boldsymbol{T}_y$ = bias, x control, and y control coefficient vectors
T = distribution matrix
$\hat{T}$ = reduced distribution matrix
T_d = dummy distribution matrix variable
U = current to force matrix
U_{x0}, U_{y0} = first derivatives of U at the center position
$U_{xx0}, U_{xy0}, U_{yx0}, U_{yy0}$ = second derivatives of U at the center position
V = current to flux density matrix
x, y = rotor displacements
$\boldsymbol{\phi}$ = magnetic flux vector
λ = Lagrange multiplier
μ_0 = permeability of air
θ = pole face angle
$(\,)^A, (\,)^B$ = bearing locations

References

[1] Lyons, J. P., Preston, M. A., Gurumoorthy, R., and Szczesny, P. M., 1994, ''Design and Control of a Fault-Tolerant Active Magnetic Bearing System for Aircraft Engine,'' *Proceedings of the Fourth International Symposium on Magnetic Bearings*, ETH Zurich, pp. 449–454.

[2] Fedigan, S. J., Williams, R. D., Shen, D., and Ross, R. A., 1996, ''Design and Implementation of a Fault Tolerant Magnetic Bearings Controller,'' *Proceedings of the Fifth International Symposium on Magnetic Bearings*, Kanazawa, Japan, pp. 307–312.

[3] Maslen, E. H., and Meeker, D. C., 1995, ''Fault Tolerance of Magnetic Bearings by Generalized Bias Current Linearization,'' IEEE Trans. Magn., **31**, No. 3, pp. 2304–2314.

[4] Maslen, E. H., Sortore, C. K., Gillies, G. T., Williams, R. D., Fedigan, S. J., and Aimone, R. J., 1997, ''A Fault Tolerant Magnetic Bearing System,'' *Proceedings of MAG'97, Industrial Conference and Exibition on Magnetic Bearings*, pp. 231–240.

[5] Maslen, E. H., Hermann, P., Scott, M., and Humphris, R. R., 1989, ''Practical Limits to the Performance of Magnetic Bearings: Peak Force, Slew Rate, and Displacement Sensitivity,'' J. Tribol., **111**, pp. 331–336.
[6] Bornstein, K. R., 1991, ''Dynamic Load Capabilities of Active Electromagnetic Bearings,'' J. Tribol., **113**, pp. 598–603.
[7] Rao, D. K., Brown, G. V., Lewis, P., and Hurley, J., 1992, ''Stiffness of Magnetic Bearings Subjected to Combined Static and Dynamic Loads,'' J. Tribol., **114**, pp. 785–789.
[8] Meeker, D. C., 1996, ''Optimal Solutions to the Inverse Problem in Quadratic Magnetic Actuators,'' Ph.D. Dissertation, Univ. of Virginia, Mechanical Engineering.
[9] Palazzolo, A. B., 1981, ''Vibrations of Locally Modified Mechanical and Structural Systems,'' Dissertation, Mechanical Engineering, University of Virginia.
[10] Keith, F. J., Williams, R. D., and Allaire, P. E., 1990, ''Digital Control of Magnetic Bearings Supporting a Multimass Flexible Rotor,'' STLE Tribol. Trans. **33**, pp. 307–314.
[11] Vance, J. M., 1988, *Rotordynamics of Turbomachinery*, Wiley Interscience.